Proceedings of the XVII ECSMGE-2019
Geotechnical Engineering foundation of the future
ISBN 978-9935-9436-1-3

doi: 10.32075/17ECSMGE-2019-0280

XVII European Conference
ECSMGE 2019
Reykjavik
on Soil Mechanics
and Geotechnical Engineering

A case study of soil-pile interaction in soft soils

Etude de cas de l'interaction sol-pieu en terrain meuble

J. Kania Corresponding / primary author
cp test a/s / Aarhus University, Vejle / Aarhus, Denmark

K. K. Sørensen
Aarhus University, Aarhus, Denmark

ABSTRACT: The results of soil-structure interaction of driven steel piles installed through soft soils are presented. Two instrumented, 12 m embedment, 406 mm diameter steel piles were installed at a construction site in Esbjerg, Denmark. One of the test piles was bitumen coated. The test piles were driven through 3.5 m of reclaimed sand and 3.6 m of soft soil into underlying sand layer. To investigate the soil-pile interaction due to pile installation and surcharge loading adjacent to the piles after installation, the test piles were instrumented with distributed fibre optic strain sensors along the full length of the piles. It was found that the test piles experienced compression loads after installation and lateral deflections due to surcharge loading in the soft soils. This case study documents the existence and magnitude of residual loads in driven steel piles after installation, the influence of bitumen coating and the effect of lateral thrust on the piles in an upper soft soil layer.

RÉSUMÉ: Les résultats de l'interaction sol-structure de pieux en acier installés au travers des terrains meubles sont présentés. Deux pieux de 406 mm de diamètre, enfouis 12m sous la surface, furent installés sur un chantier à Esbjerg au Danemark. L'un des pieux tests était enduit de bitume. Les pieux tests furent battus à travers 3,5 m de sable de récupération et 3,6 m de terre meuble avant d'atteindre une couche de sable sous-jacente. Afin d'examiner l'interaction entre le sol et le pieu après son installation et l'effet de surcharge adjacente aux pieux après cette même installation, les pieux tests furent équipés de senseurs en fibre optique distribués sur toute leur longueur. Il a ainsi été découvert que les pieux tests subissaient des forces de compression après installation, entraînant des déviations causées par l'effet de surcharge en terrain meuble. Cette étude de cas rend compte : de l'existence et de l'ampleur de charges résiduelles sur des pieux en acier battus après leur installation : de l'influence du revêtement bitumineux, et également de l'effet de poussée latérale sur les pieux au sein d'une couche supérieure de terrain meuble.

Keywords: residual load, lateral soil movement, bitumen coating, distributed fibre-optic sensors

INTRODUCTION

The function of piles is generally to transfer load from a structure through soft compressible soil layers to stiffer or less compressible soils. Soil-pile interaction involves a combination of vertical and horizontal loads. An example of vertical load is residual load. Residual load in a driven pile is the axial load present in a pile after its installation. For each hammer blow a negative skin friction develops in the upper part of a driven pile and a positive shaft resistance in the lower part, due to the pile's upward movement during a rebound. The point of equilibrium exists where the shaft resistance reverse from negative direction to positive direction (Briaud and Tucker 1984,

Fellenius 2015). Horizontal loads occur when piles are installed in a soft soil layer which deforms increasing horizontal pressures. As a consequence bending moments develop in the piles and the piles experience deflections (Poulos 1973, Springman and Bolton 1990).

The test setup was designed to investigate negative skin friction under uniform loading. Unfortunately, due to construction activities an unplanned one-sided loading occurred, which affected the test site. This paper will focus on the residual load apparent after driving a steel pile with and without bitumen coating and deflections of the test piles due to surcharge loading adjacent to the piles.

This paper first gives details of the site conditions and the instrumentation of the test setup. The presentation and discussion of results will focus on the examination of the residual load on an uncoated and coated driven steel pile and the deflections due to one sided surcharge loading.

2 MATERIALS AND METHODS

2.1 Site conditions

The test site is located in Esbjerg, Denmark. At the site land was reclaimed from the sea by placing fill up to +4.5 m above sea level (ASL) to construct a new harbour. The ground profile consists of 3.5 m thick reclaimed uniform, fine to coarse sand fill layer on top of 3.6 m soft soil layer overlying a postglacial marine, dense, uniform, medium sand layer. Based on the previous site investigation carried out by GEO (GEO 2016) and Jysk Geotekinik (JyskGeoteknik 2017) and testing carried out on samples collected in connection to the installation of in-situ monitoring equipment for the test setup, the soft soil layer is found to be of postglacial marine origin, highly organic and consisting of gyttja (at roughly 3.5-4.3 m depth) and peat (at roughly 4.3-7.1 m depth). The gyttja layer is characterized by an average water content of 61 %, an average plastic limit of 55 % and an average liquid limit of 136 %. The peat layer is characterized by an average water content of 285 %, an average plastic limit 256 % and an average liquid limit of 373 %. Based on the oedometer tests, the soft soil layer is normally consolidated. According to CPT sounding and the empirical approaches available for interpretation of undrained shear strength from CPT (Lunne, Robertson et al. 1997), the average undrained shear strength of soft soil layer is equal to 16 kPa (assuming the empirical cone factor N_k equal to 15).

2.2 Test setup and instrumentation

The test setup is illustrated in Figure 1. The setup consisted of four instrumented test piles and in-ground monitoring of water pressure and settlement.

Two instrumented Ø 406 diameter (8 mm wall thickness) steel test piles (with and without bitumen coating) and the two instrumented 350 mm x 350 mm square precast concrete piles (with and without bitumen coating) were driven to the approximate depth of 12 m by a Hitachi 180-3 piling rig with a 90 kN Junttan HHK9A hammer.

The instrumentation and the obtained results from concrete test piles will not be described in this paper due to malfunctioning of one of the installed strain distributed fibre optic sensors (DFOS).

All of the instrumentation and the test piles were installed from a working platform (0.0 m depth) at 1.5 m ASL. The test piles were installed in December 2017 and the field instrumentation was installed in January 2018.

To measure pore water pressure low air entry vibrating wire piezometers were installed at 5.0, 6.5, 7.7, and 12.2 m depth using the fully grouted installation method. The grout consisted of water, cement and bentonite with the 8:1:1 ratio by

weight (water:cement:bentonite). A stand pipe was installed with an intake zone at 12.5 m depth.

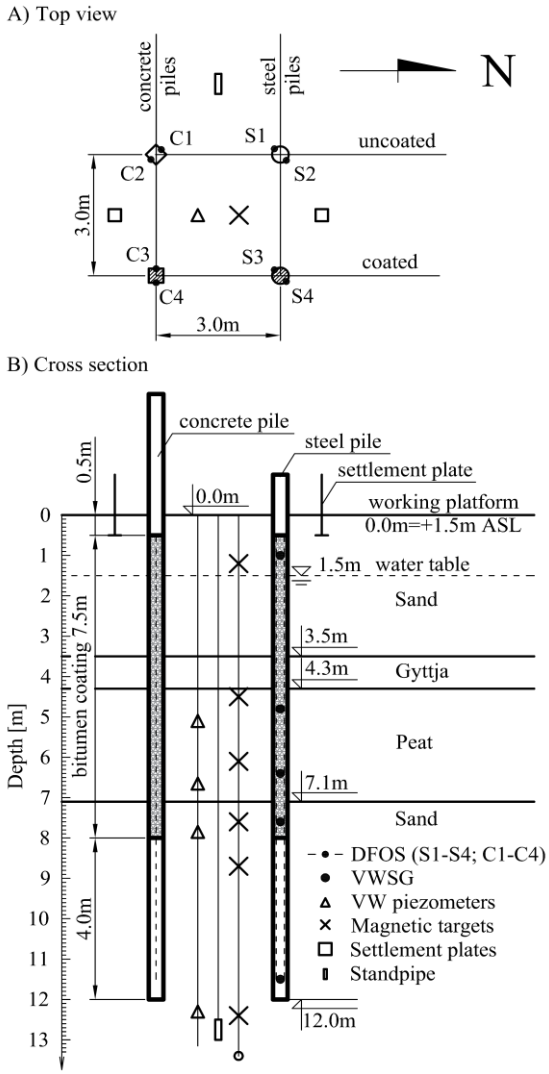

Figure 1. Soil profile and the test setup.

The settlement of the surface was measured by two settlement plates installed at 0.5 m depth, while the settlements at different depths were monitored by magnetic extensometers. The six magnetic targets (6 leaf spider magnets) and the datum magnet were installed at 1.2, 4.4, 6.1, 7.6, 8.7, 12.4, and 13.4 m depth respectively.

The steel test piles were instrumented with two opposite mounted strain distributed fibre optic sensors (DFOS). As presented in Figure 2, Brusens V9 cables were used as strain DFOS. All DFOS were placed along a welded (one side chain intermittent) Ø12mm steel rebar, pre-strained to about 1000με and glued using Araldite 2012 epoxy. Additionally, both steel test piles were equipped with one set of vibrating wire strain gauges (VWSG) installed at five different depths: 1.0, 4.8, 6.4, 7.6 and 11.5 m respectively on each steel pile. The VWSG were protected by welded on angle iron. One of the steel test piles was coated along 7.5 m (0.5-8.0 m depth) with a 1 mm thick, 80/100 penetration bitumen coating. Both steel piles were supplied with point-end pile shoe.

Figure 2. Installation of strain DFOS on the steel piles.

2.3 Temperature compensation of strain measurements

An optical distributed sensor interrogator based on Rayleigh scattering was used in this case study. The principle of Rayleigh-based distributed fibre-optical sensing techniques was presented in previous studies (Palmieri and Schenato 2013). Similar to strain gauges, fibre optic strain sensors mounted on a test object are sensitive to mechanically and thermally induced strain (Luna 2014).

Unfortunately, it was revealed before installation of the test piles that temperature DFOS was

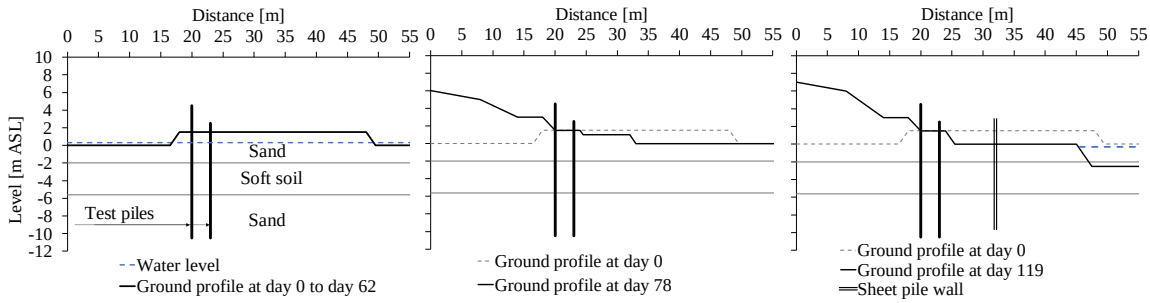

Figure 3. Construction activities around the test setup at selected days after installation of piles.

malfunctioning. To obtain temperature distribution with depth the temperature readings (at the depths of installation) were collected from the VWSGs and the interpolation between measuring points was made. Then the mechanical strains were obtained using the equation as given below:

$$\varepsilon_m^z = \varepsilon_t^z + \left(0{,}95 \cdot \frac{\Delta T^z}{k_T} \cdot k_\varepsilon + \Delta T^z \cdot \alpha_L\right) \quad (1)$$

Where ε_m^z (με) is mechanical strain at depth z, ε_t^z (με) is total (measured) strain at depth z, ΔT^z (°C) is change in temperature at depth z, k_T (°C/GHz) is temperature conversion factor equal to -0.638 °C/GHz, k_ε (με/GHz) is strain conversion factor equal to -6.67 με/GHz, α_L is thermal expansion coefficient of steel assumed in this study as 12.2 με/°C.

2.4 Expected distribution of residual load

In order to evaluate the measured distribution of residual load on uncoated and coated driven steel test pile estimations were made using commercially available GRLWEAP software. The modelling parameters are presented in Table 1. The Alm and Hamre (Alm and Hamre, 2002) soil model and standard skin and toe quake and damping parameters were used. Based on driving logs a 20 cm hammer stroke and 25 and 19 blow counts for every 20 cm at the end of driving the uncoated and coated pile were used respectively.

Table 1. Modelling parameters of soil layers

Soil type	**γ/γsat** kN/m³	**Surface friction** °	**Cu** kPa
Sand	18/20	28 – uncoated 28 - coated	-
Gyttja	16	-	16
Peat	11	28 – uncoated 15 - coated	-

2.5 History of construction activities around the test setup

Main construction activities around the test setup consisted of filling the area with reclaimed sand up to 4.5 m ASL and the installation of an anchored sheet pile wall for the new harbour. It can be seen from the sketches in Figure 3 that the major change took place 78 days after installation of the test piles, when the area at only one side (South side) was filled up to around +6.0 m ASL. This area was continuously filled with reclaimed sand until 119 days after installation of piles. Based on the author's field observations, the sheet pile wall near the test setup was completed around 91 days after installation of piles.

RESULTS

As mentioned in 2.2, only results obtained from the steel test piles are presented in this paper. In all figures negative values denote compression loads and positive values denote tension loads.

To smoothen the strain profiles, a moving average of 100 consecutive reading was used to present data obtained from DFOS (giving a virtual gauge length of roughly 0,26 m located every 2.6 mm).

3.1 Residual loads and deflection of the test piles after driving

The measured strain distribution of opposite mounted strain DFOS on the uncoated and coated steel test piles after installation of the piles are presented in Figure 4 and Figure 5 respectively. From the data in Figure 4 it appears that the uncoated steel test pile experienced arc-shape deflection after driving, since the opposite sensors are located at the opposite sides of the average along the full length.

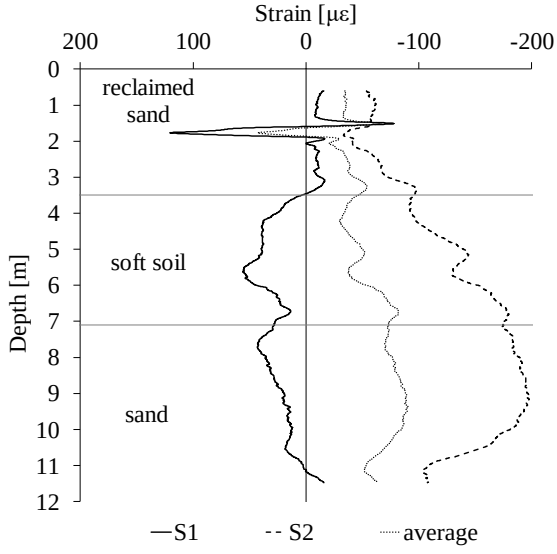

Figure 4. Measured strain distribution of opposite mounted DFOS on the uncoated steel test pile after pile installation

In contrast to the observed strain distribution of the uncoated pile, Figure 5 shows that the strain distribution of the coated steel test pile experienced S-shape deflection after driving with the intersection point located at approximately 4.7 m depth.

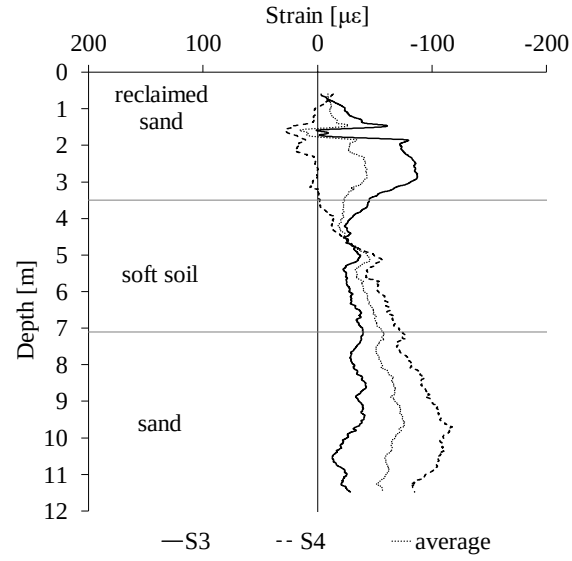

Figure 5. Measured strain distribution of opposite mounted distributed fibre optic sensor on the coated steel test pile after pile installation

The residual loads for the uncoated and coated steel test pile are presented in Figure 6 and Figure 7 respectively. The load distribution obtained from DFOS for each test pile was calculated based on averaging measured strain distributions of opposite mounted strain DFOS sensors and assuming the Young's modulus of steel equal to 210 GPa.

As shown in Figure 6 the residual load on the uncoated steel test pile obtained from DFOS and GRLWEAP reaches its maximum compression value of 190 kN (at 9.4 m depth) and 127 kN (at 8,0 m depth) respectively. The average unit shaft resistance within soft soil layer (3.5-7.1 m depth) is 30 kPa and 10 kPa obtained from DFOS and GRLWEAP respectively.

As shown in Figure 7 the residual load on the coated steel test pile obtained from DFOS and GRLWEAP reaches its maximum compression value of 160 kN (at 9.6 m depth) and 100 kN (at 8,0 m depth) respectively. The average unit shaft resistance within soft soil layer (3.5-7.1 m depth) is 19 kPa and 6 kPa obtained from DFOS and GRLWEAP respectively.

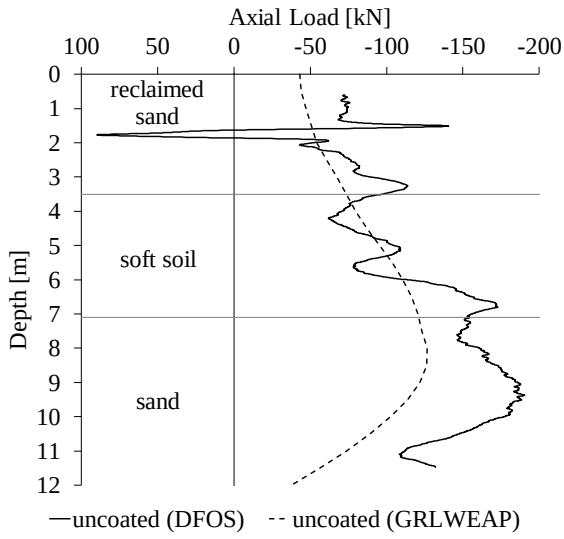

Figure 6. Residual load distribution on the uncoated steel test pile obtained from DFOS and GRLWEAP

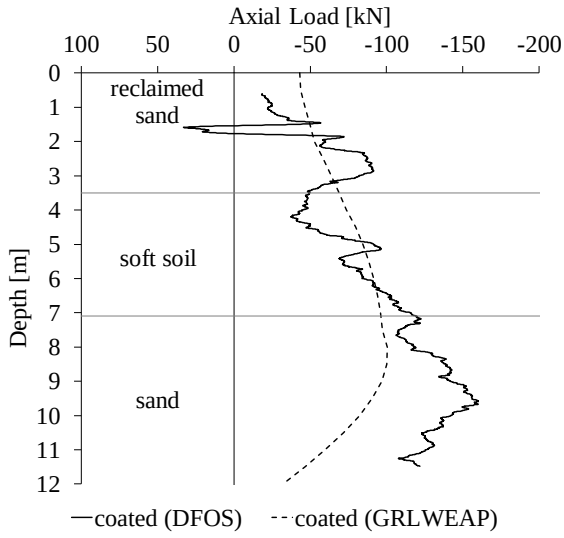

Figure 7. Residual load distribution on the coated steel test pile obtained from DFOS and GRLWEAP

3.2 The influence of surcharge loading adjacent to the test piles

To assess the influence of one sided surcharge loading adjacent to the test piles, the strain distributions were used. Figure 8 and Figure 9 present the measured strain distributions of opposite mounted distributed fibre optic strain sensors on the uncoated and coated steel test piles respectively at selected days after pile installation.

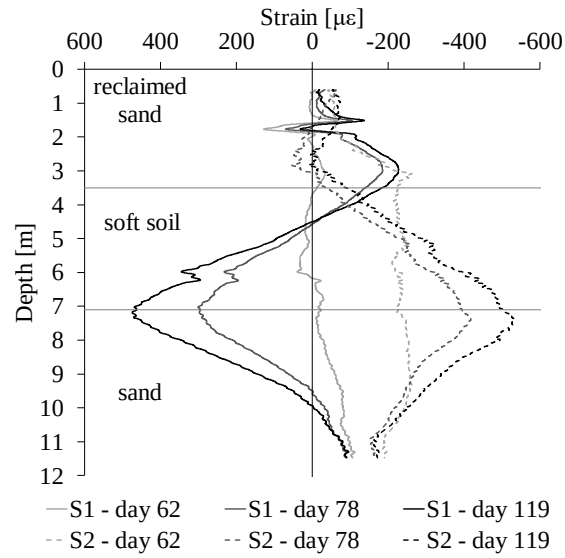

Figure 8. Measured strain distribution of opposite mounted DFOS on the uncoated steel test pile at selected days after pile installation

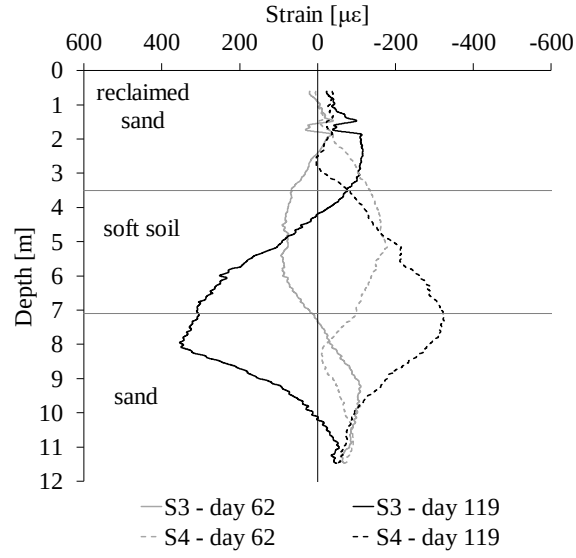

Figure 9. Measured strain distribution of opposite mounted DFOS on the coated steel test pile at selected days after pile installation

As shown in Figure 8, there was a significant difference between strain profiles obtained at day

62 and 78 after installation of the piles. The strain profiles obtained from the sensor S1 and S2 62 days after installation of piles indicate arc-shape deflection of the uncoated pile. At day 78 and later (day 119) the strain profiles indicate an S-shape deflection of the uncoated pile having an intersection point located around 4m depth and two local maximum tension and compression values located around 3.0 and 7.5 m depth. The strain profiles presented in Figure 9 indicate a deflection change of the coated pile. At day 62 the coated pile experienced an S-shape deflection with an intersection point at 8 m depth. At day 119 the deflection type was still S-shaped, however the intersection point had shifted to 3.5 m depth. The local maximum tension and compression values were located at the former intersection point around 8.0 m depth. Interestingly, above 3.5 m depth (intersection point at day 119) and below 8m depth (intersection point at day 62) the individual sensors S3 and S4 reversed its position e.g. S3 from tension to compression side at the top and from compression to tension side at the bottom.

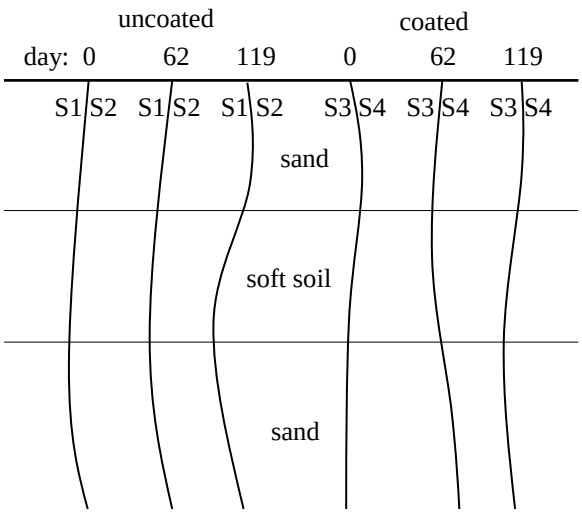

Figure 10. Sketch of deflection of the uncoated and coated pile at selected days after piles installation based on measured strain profiles

The deflection history of the test piles, based on the measured strain distribution is provided in Figure 10. It is important to note that the piles experienced additional compression loads due to residual loads and soil settlement.

DISCUSSION

Prior studies have noted the importance of residual load (Poulos 1987, Kim, Chung et al. 2011) and lateral thrust (Davisson 1970, Springman and Bolton 1990) to understand and properly assess soil-pile interaction. This study confirms the existence of residual load after driving steel piles and deflection of piles due to one sided surcharge loading.

In this case study the distributed fibre optic sensing interrogator based on Rayleigh scattering was used. Due to its spatial resolution (2.6 mm), very detailed strain profiles were obtained and characteristic points were precisely located. Unfortunately, the test setup did not involve inclinometers to monitor lateral soil movement, since the test setup was designed to investigate negative skin friction. Also, the test piles would have benefitted from having two pairs of diametrically opposite strain DFOS to locate the neutral axis and direction of bending. Additionally, at least one more temperature DFOS should be mounted as a backup.

The obtained residual load distributions are consistent with other studies which found that a negative skin friction is building up in the upper portion of a pile and a positive shaft resistance develops in the lower portion of a pile. The maximum residual loads obtained from DFOS were higher than obtained from GRLWEAP for the uncoated and coated steel test pile by 50 % and 60 % respectively. The maximum value of residual load obtained from DFOS and GRLWEAP on the coated steel test pile was smaller than on the uncoated pile. This finding suggests that bitumen coating reduces the residual load.

Interestingly, the point of equilibrium between negative skin friction and positive shaft resistance after driving for uncoated and coated steel test pile was located around the same depth. However, it was located deeper for DFOS (9.5 m depth) than GRLWEAP (8.0 m depth).

The consequence of not considering the presence of residual load will lead to overestimating the shaft resistance along the upper section and underestimating the shaft resistance along the lower section of the pile (Fellenius 2015).

The assumed deflection of piles, based on measured strain profiles, supports previous research regarding passive lateral thrust on piles. It can therefore be assumed that these factors (residual load and lateral thrust) can affect any further measurements of soil-pile interaction e.g. negative skin friction.

CONCLUSION

This case study has shown that:

1) Residual load is present after installation of a driven steel pile with and without bitumen coating.

2) Bitumen coating reduces the magnitude of residual load, but it does not change the point of equilibrium between negative skin friction and positive shaft resistance.

3) Surcharge loading adjacent to piles installed through soft soils causes deflection of piles.

4) DFOS can be successfully installed on driven steel piles.

5) The instrumentation of a test setup to monitor soil-pile interaction located on ongoing construction site should be carefully planned.

ACKNOWLEDGEMENTS

The authors would like to thank cp test a/s, Per Aarsleff A/S, Centrum Pæle A/S, DMT Gründungstechnik GmbH and Innovation Fund Denmark for providing funding for this study and Per Aarsleff A/S for providing data and for installing the instrumented test piles.

REFERENCES

Alm, T., Hamre, L. 2002. Soil model for pile driveability predictions based on CPT interpretations. *Proceedings of The International Conference on Soil Mechanics and Geotechnical Engineering* **2**, 1297-1302, AA Balkema Publishers.

Briaud, J.-L., Tucker, L. 1984. Piles in sand: a method including residual stresses. *Journal of Geotechnical Engineering* **110**, 1666-168.

Davisson, M. 1970. Lateral load capacity of piles. *Proceedings: 49th Annual Meeting of the Highway Research Board*, 104-112, Washington District of Columbia, United States.

Fellenius, B. H. 2015. Static tests on instrumented piles affected by residual load. *DFI Journal - The Journal of the Deep Foundations Institute* **9**, 11-20.

GEO. 2016. *Esbjerg Strand, Laboratorieforsøg*.

JyskGeoteknik. 2017.*Geoteknisk Datarapporter*.

Kim, S. R., Chung, S. G., Fellenius, B. H. 2011. Distribution of residual load and true shaft resistance for a driven instrumented test pile. *Canadian Geotechnical Journal* **48**, 583-598.

Luna. 2014. *Distributed Fiber Optic Sensing: Temperature Compensation of Strain Measurement* (EN-FY1402).

Lunne, T., Robertson, P., Powell, J. 1997. *Cone penetration testing in geotechnical practice*. Spon Press, Abingdon.

Palmieri, L., Schenato, L. 2013. Distributed optical fiber sensing based on Rayleigh scattering. *The Open Optics Journal* **7**, 104-127.

Poulos, H. G. 1973. Analysis of piles in soil undergoing lateral movement. *Journal of Soil Mechanics & Foundations Div* **99**, 391-406.

Poulos, H. G. 1987. Analysis of residual stress effects in piles. *Journal of Geotechnical Engineering* **113**, 216-229.

Springman, S., Bolton, M. 1990. *The effect of surcharge loading adjacent to piles*, Transport and Road Research Laboratory (TRRL), Wokingham, Berkshire, United Kingdom.